

AD-A115 930

BOLT BERANEK AND NEWMAN INC CAMBRIDGE MA  
INTERFEROMETRIC DETECTION OF ULTRASOUND. (U)  
JUL 81 M J RUDD

F/6 20/1

UNCLASSIFIED

BBN-4699

NADC-79009-60

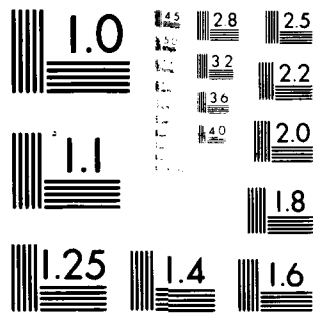
N62269-80-C-0260

NL

1-1  
40  
120



END  
DATE  
FILMED  
7-82  
DTIC



MICROCOPY RESOLUTION TEST CHART

AD A115930



12

REPORT NO. NADC-79009-60

INTERFEROMETRIC DETECTION OF ULTRASOUND

MICHAEL J. RUDD

PREPARED BY

BOLT BERANEK AND NEWMAN INC.  
CAMBRIDGE, MA 02238

FINAL REPORT

1 JULY 1981

APPROVED FOR PUBLIC RELEASE: DISTRIBUTION UNLIMITED

FILE COPY

PREPARED FOR  
NAVAL AIR DEVELOPMENT CENTER  
WARMINSTER, PENNSYLVANIA  
CONTRACT NO. N62269-80-C-0260

JUL 23 1982

A

01

## NOTICES

REPORT NUMBERING SYSTEM - The numbering of technical project reports issued by the Naval Air Development Center is arranged for specific identification purposes. Each number consists of the Center acronym, the calendar year in which the number was assigned, the sequence number of the report within the specific calendar year, and the official 2-digit correspondence code of the Command Office or the Functional Directorate responsible for the report. For example: Report No. NADC-78015-20 indicates the fifteenth Center report for the year 1978, and prepared by the Systems Directorate. The numerical codes are as follows:

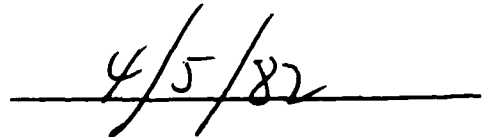
CODE	OFFICE OR DIRECTORATE
00	Commander, Naval Air Development Center
01	Technical Director, Naval Air Development Center
02	Comptroller
10	Directorate Command Projects
20	Systems Directorate
30	Sensors & Avionics Technology Directorate
40	Communication & Navigation Technology Directorate
50	Software Computer Directorate
60	Aircraft & Crew Systems Technology Directorate
70	Planning Assessment Resources
80	Engineering Support Group

PRODUCT ENDORSEMENT - The discussion or instructions concerning commercial products herein do not constitute an endorsement by the Government nor do they convey or imply the license or right to use such products.

APPROVED BY:

  
J. R. WOODS  
CDR USN

DATE:



REPORT DOCUMENTATION PAGE		READ INSTRUCTIONS BEFORE COMPLETING FORM
1. REPORT NUMBER NADC-79009-60	2. GOVT ACCESSION NO. AD-A225 930	3. RECIPIENT'S CATALOG NUMBER
4. TITLE (and Subtitle) Interferometric Detection of Ultrasound	5. TYPE OF REPORT & PERIOD COVERED Final Report, 1 September 1980 - 1 July 1981	
	6. PERFORMING ORG. REPORT NUMBER 4699	
7. AUTHOR(s) M. J. Rudd	8. CONTRACT OR GRANT NUMBER(s) N62269-80-C-0260	
9. PERFORMING ORGANIZATION NAME AND ADDRESS Bolt Beranek and Newman Inc. 10 Moulton Street Cambridge, MA 02138	10. PROGRAM ELEMENT, PROJECT, TASK AREA & WORK UNIT NUMBERS	
11. CONTROLLING OFFICE NAME AND ADDRESS Naval Air Development Center Warminster, PA 18974	12. REPORT DATE July 1981	
	13. NUMBER OF PAGES 36	
14. MONITORING AGENCY NAME & ADDRESS (if different from Controlling Office) Naval Air Development Center Warminster, PA 18974 Attention: (Code 6063)	15. SECURITY CLASS. (of this report) Unclassified	
	15a. DECLASSIFICATION/DOWNGRADING SCHEDULE	
16. DISTRIBUTION STATEMENT (of this Report)  APPROVED FOR PUBLIC RELEASE; DISTRIBUTION UNLIMITED		
17. DISTRIBUTION STATEMENT (of the abstract entered in Block 20, if different from Report)		
18. SUPPLEMENTARY NOTES		
19. KEY WORDS (Continue on reverse side if necessary and identify by block number) Laser, Interferometer, Heterodyne, Ultrasound Non-Destructive Testing, Ultrasonics		
20. ABSTRACT (Continue on reverse side if necessary and identify by block number) This report describes the development of an interferometer to measure ultrasonic surface vibrations. The output from a low power helium-neon laser was focused onto the surface to be measured, and the phase of the reflected light was measured. The type of interferometer used was an Optical Heterodyne Interferometer, in which the frequency of the reference beam was shifted by 40 MHz and a phase-locked loop was built to track the 40-MHz signal.		

Unclassified

SECURITY CLASSIFICATION OF THIS PAGE (When Data Entered)

The sensitivity, frequency response, and pulse response were measured and compared with those from a PZT transducer. The effects of different surface finishes were also studied, and the sensitivity was compared with theoretical values. The actual sensitivity was  $15\text{\AA}$  on a 10-MHz bandwidth, and  $2 \times 10^{-2}\text{\AA}$  on a 1-Hz bandwidth. Finally, suggestions are made to improve the sensitivity still further.

0.021  
=

Unclassified

SECURITY CLASSIFICATION OF THIS PAGE (When Data Entered)

NADC-79009-60



D 110  
80PK  
INSPECTED  
2

ABSTRACT

This report describes the development of an interferometer to measure ultrasonic surface vibrations. The output from a low power helium-neon laser was focused onto the surface to be measured, and the phase of the reflected light was measured. The type of interferometer used was an Optical Heterodyne Interferometer, in which the frequency of the reference beam was shifted by 40 MHz and a phase-locked loop was built to track the 40-MHz signal.

The sensitivity, frequency response, and pulse response were measured and compared with those from a PZT transducer. The effects of different surface finishes were also studied, and the sensitivity was compared with theoretical values. The actual sensitivity was  $15\text{\AA}$  on a 10-MHz bandwidth, and  $2 \times 10^{-2}\text{\AA}$  on a 1-Hz bandwidth. Finally, suggestions are made to improve the sensitivity still further.

TABLE OF CONTENTS

	Page
ABSTRACT .....	iii
LIST OF FIGURES .....	v
LIST OF TABLES.....	vi
SECTION 1. INTRODUCTION .....	1
2. DEVELOPMENT OF THE LASER VIBROMETER .....	2
2.1 Principle of Operation .....	2
3. COHERENCE .....	7
4. LASER VIBROMETER SENSIVITY .....	9
5. FREQUENCY RESPONSE OF LASER VIBROMETER .....	11
6. PULSE RESPONSE OF LASER VIBROMETER .....	13
7. COMPARISON WITH PZT .....	16
8. EFFECTS OF SURFACE FINISH ON SIGNAL-TO-NOISE RATIO .....	18
9. THEORETICAL PERFORMANCE OF THE OPTICAL SYSTEM ..	20
10. IMPROVEMENTS IN SENSITIVITY .....	23
11. CONCLUSIONS .....	24
APPENDIX A: DESIGN OF THE PHASE TRACKER .....	A-1

LIST OF FIGURES

	Page
FIGURE 1. Optical System .....	3
2. Illumination on Photodiode in Correct Alignment .....	6
3. Variation of Signal Level with Path Length .....	8
4. Noise Level of Laser Vibrometer .....	10
5. Frequency Response of Laser Vibrometer Measuring a PZT Transducer .....	12
6. Pulse Response of Laser Vibrometer .....	14
7. Pulse Response of 10 MHz PZT Transducer .....	15
8. Frequency Response of PZT Transducer .....	17
A.1. Block Diagram of the Phase Tracker .....	A-2

LIST OF TABLES

	Page
Table I. Signal Strength as a Function of Surface Finish (Signal Levels mv rms.).....	19
II. Photodiode Noise (300 mv = Full Scale = 158.2 nm or 5.27 A/mv) .....	21

1. INTRODUCTION

For many years, ultrasonic surface vibrations have been measured with piezoelectric transducers. However, at a frequency of 10 MHz, the wavelength of the ultrasound is about 0.5 mm, and the transducer may be 12 mm in diameter. This size makes the transducer very directional, and it may have an erratic response if the coupling is not uniform. Further, the mass, or rather the impedance, of the transducer can modify the response of the surface.

The solution to this problem is to use a transducer of very small diameter (less than 0.5 mm) and very small impedance, or an optical transducer. A laser beam focused on the surface to be measured is such a transducer. An optical transducer also has a tremendous advantage: It can be readily scanned across the surface by simply moving a mirror.

Work is proceeding independently on the use of a laser source to generate the ultrasonic waves. The use of an optical detector complements the optical generator of sound.

## 2. DEVELOPMENT OF THE LASER VIBROMETER

### 2.1 Principle of Operation

The Laser Vibrometer is able to measure very small-amplitude high-frequency vibrations. The amplitudes can be a small fraction of an Angstrom up to a quarter of a wavelength of light ( $1582 \text{ \AA}$ ). This is achieved by an Optical Heterodyne Interferometer (Fig. 1). Light scattered from the vibrating surface is caused to interfere with a reference beam. This beam has been shifted in frequency, giving a carrier frequency of 40 MHz. This frequency shift eliminates problems of thermal drift of the interferometer. The amplitude of the vibration is determined by measuring the phase modulation of the 40-MHz carrier. The signal processor puts out an analog signal proportional to the vibration displacement.

The whole optical system is mounted on an optical bench. It includes a laser; an Acousto-Optic Modulator, which is screwed onto the end; a Dove prism to fold the laser beam; a microscope lens on a translation stage to focus the laser beam on the target; a separating mirror M and a silicon avalanche photodiode and preamplifier. The power applied to the Acousto-Optic Modulator is a maximum so that most of the optical power is in the beam shifted by 40 MHz. This eliminates problems with optical feedback. The main beam is centered on the microscope objective, which focuses it on the target. The reflected light retraces the path and is reflected off the laser end mirror. It then combines with the weaker beam, which is separated by the mirror M and falls on the photodiode. The photodiode generates a 40-MHz output that is phase-modulated in the same way as the optical beam.

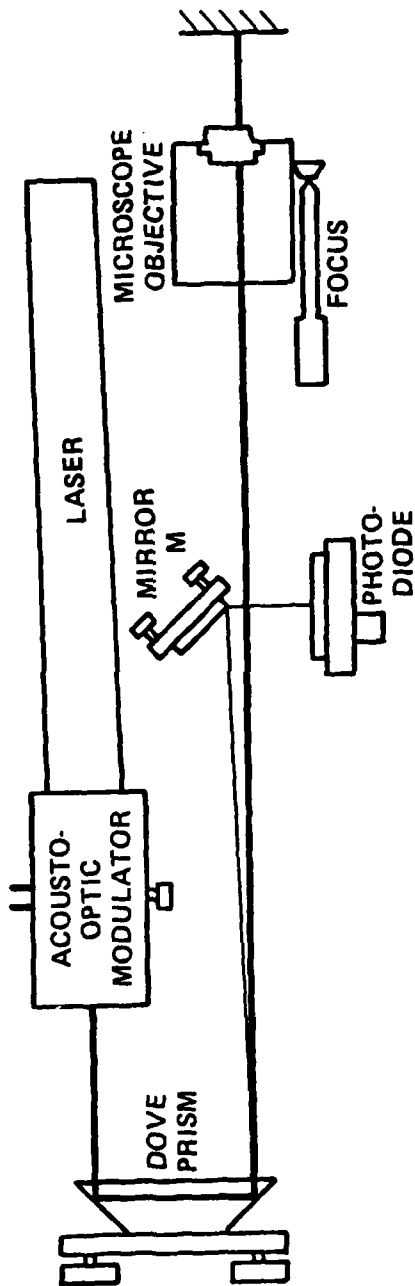


FIGURE 1. OPTICAL SYSTEM.

Two main problems emerged in developing the optical system. These were

1. Optical feedback into the laser cavity.
2. Noise due to spurious scattered light.

At first optical feedback into the laser was a serious problem. The light that was backscattered from the target reentered the laser cavity and amplitude-modulated the output. Only a small amount of light was required to obtain 100% amplitude modulation. This caused the phase-locked loop periodically to lose lock. Rotation of the plane of polarization was attempted, using a quarter-wave plate, so that the returned light could not interfere with the original light. However, this did not produce sufficient suppression.

The solution proved to be very simple. We require very little light on the photodiode; most of the light goes to the target surface. Initially we used very little power on the modulator, so that most optical power went to the surface. However, we can invert the situation and apply maximum power to the modulator. Then most of the optical power is in the frequency-shifted beam, and very little in the unshifted beam. If light from the target is scattered back into the laser cavity, it is shifted in frequency. The laser cavity has a bandwidth of only 1 MHz. If the returned light is shifted by more than this, then the laser will not respond. This indeed proved to be the case, and optical feedback was no longer a problem.

The other problem, noise due to spurious scattered light, was more subtle. Light is typically scattered by dirt and small imperfections on the optical surfaces. These can be minimized but not eliminated by careful cleaning with alcohol and a soft tissue. This scattered light usually will be both unshifted and shifted by 40 MHz. The frequency-shifted light will beat with the unshifted reference beam to produce a spurious 40-MHz signal. On the original optical scheme, the reflected light passed through the modulator again and was shifted by another 40 MHz, so that the beat signal was 80 MHz, which could be separated from the 40-MHz scattered light signal. However, problems were encountered. First, the 40-MHz signal was much stronger than the 80-MHz signal, causing problems in the limiter and multiplier. Second, when a diffuse target surface, rather than a mirror was used, the returned wavefront was corrugated and was not at the right angle to be frequency-shifted again. Hence the signal of interest is really 40 MHz and not 80 MHz, and the spurious signal and the signal of interest are at the same frequency. This obstacle at first seemed to be insurmountable.

It has been found, however, that by adjusting the photodiode through the mirror M, a "sweet spot" can be detected. At this position (see Fig. 2) the noise is a minimum and the signal is a maximum. This position is slightly to one side of the unshifted beam.

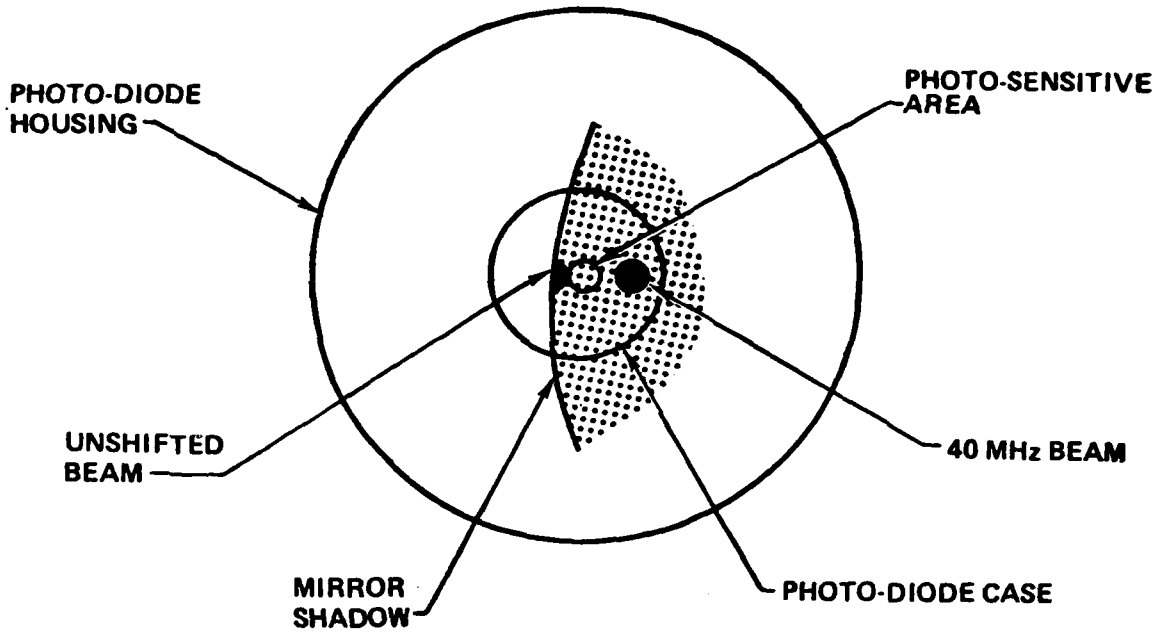


FIGURE 2. ILLUMINATION OF PHOTODIODE IN CORRECT ALIGNMENT.

### 3. COHERENCE

The laser actually does not oscillate at only one frequency, but at three or four frequencies, separated by  $C/2L$ , where  $L$  = laser cavity length and  $C$  = speed of light. For this particular laser, the cavity length is  $13\text{-}3/4$  in. and the mode spacing is 464 MHz. In general, these different modes will have different phases. When added together in an interferometer, they will give beat signals of different phases and tend to cancel out each other. However, they are all in phase on the laser end mirror and again at distances  $L$ ,  $2L$ ,  $3L$ , etc., from the laser end mirror. Hence in the Optical Heterodyne Interferometer the distance from the laser end mirror to the target must be an integral number of cavity lengths, namely  $13\text{-}3/4$ ,  $27\text{-}1/2$ ,  $41\text{-}1/4$ , etc., inches. Typically there is a tolerance of  $\pm 3$  in. in the allowable position. If the target position does not meet these criteria, the heterodyne signal may be as much as 20 dB less than the optimum. The variation of signal level with path length is shown in Fig. 3. This difficulty can be eliminated by using a single mode laser, such as the Tropel model.

The optical path length to the end of the Acousto-Optic Modulator and inside the Dove prism is partly in glass, which has a 50% greater optical path length than geometrical path length (refractive index of 1.5). The total path length of the two components is 10 in. with  $3\text{-}1/2$  in. between them, totaling  $13\text{-}1/2$  inches. Thus the target should be  $27\text{-}3/4$  in. from the face of the Dove prism.

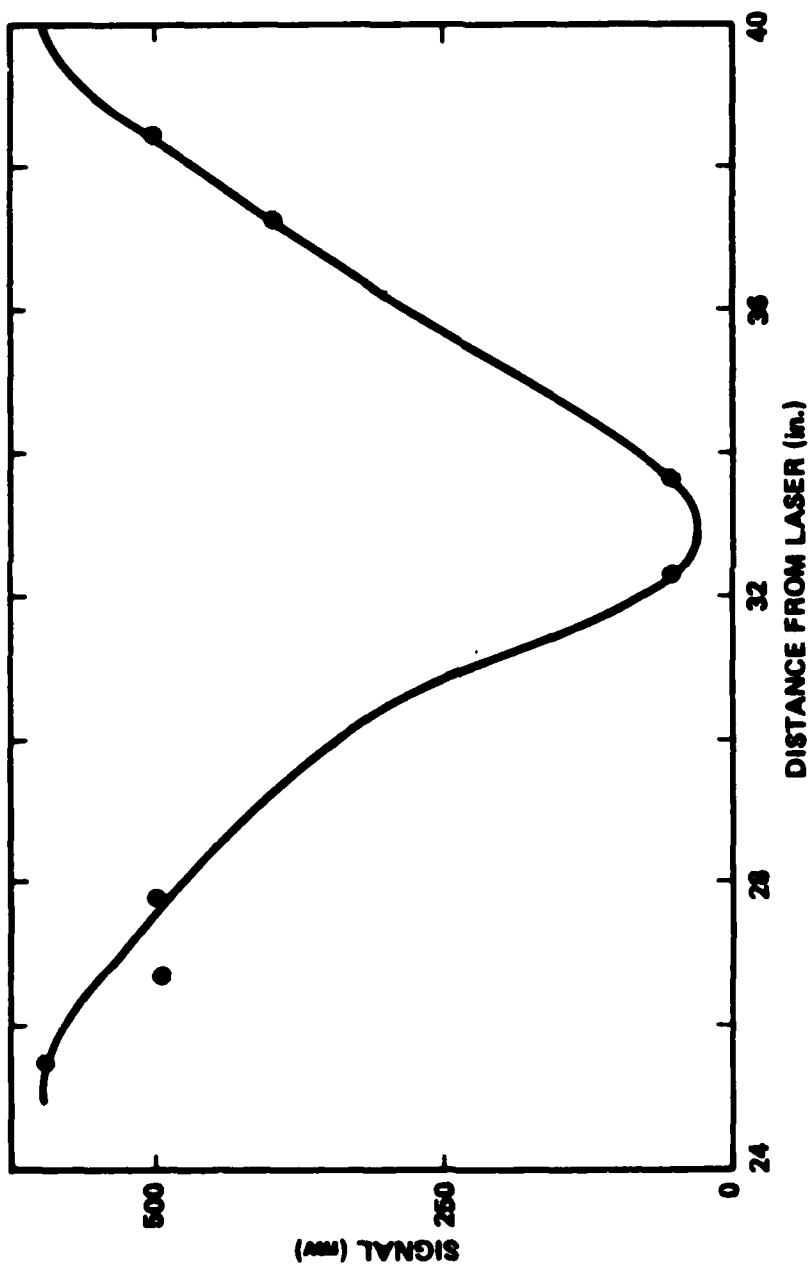


FIGURE 3. VARIATION OF SIGNAL LEVEL WITH PATH LENGTH.

## 4. LASER VIBROMETER SENSITIVITY

The sensitivity of the Laser Vibrometer is characterized by its noise floor on a given bandwidth. This noise level, a 1-Hz bandwidth, is shown as a function of frequency in Fig. 4. The noise was measured with a PAR Lock-In Amplifier tuned to a particular frequency. The integration time was 0.1 sec corresponding to a 1.6-Hz bandwidth. The results were divided by 1.26 to produce Fig. 4. The 10-MHz bandwidth shot-noise level gives displacement noise of  $15 \text{ \AA}$  rms, which is only about 1,000 times the level of the 1-Hz noise. With a 10-MHz bandwidth we would expect a level 3,000 times greater. This means that the 1-Hz levels may be really lower than measurements indicate, and that the measured noise is partly due to noise or pick-up in the Lock-In Amplifier.

If the noise is truly "white" then its power is proportional to its bandwidth or its voltage is proportional to the square root of the bandwidth. Thus the equivalent noise for the displacement is proportional to the square root of the bandwidth (BW). Thus

$$\text{Equivalent displacement noise} \approx .015 (\text{BW})^{1/2} \text{ \AA}$$

$$\text{For an averaging time } t, \quad \text{BW} = 1/2\pi t \text{ and}$$

$$\text{Equivalent displacement noise} \approx .006/t^{1/2} \text{ \AA}.$$

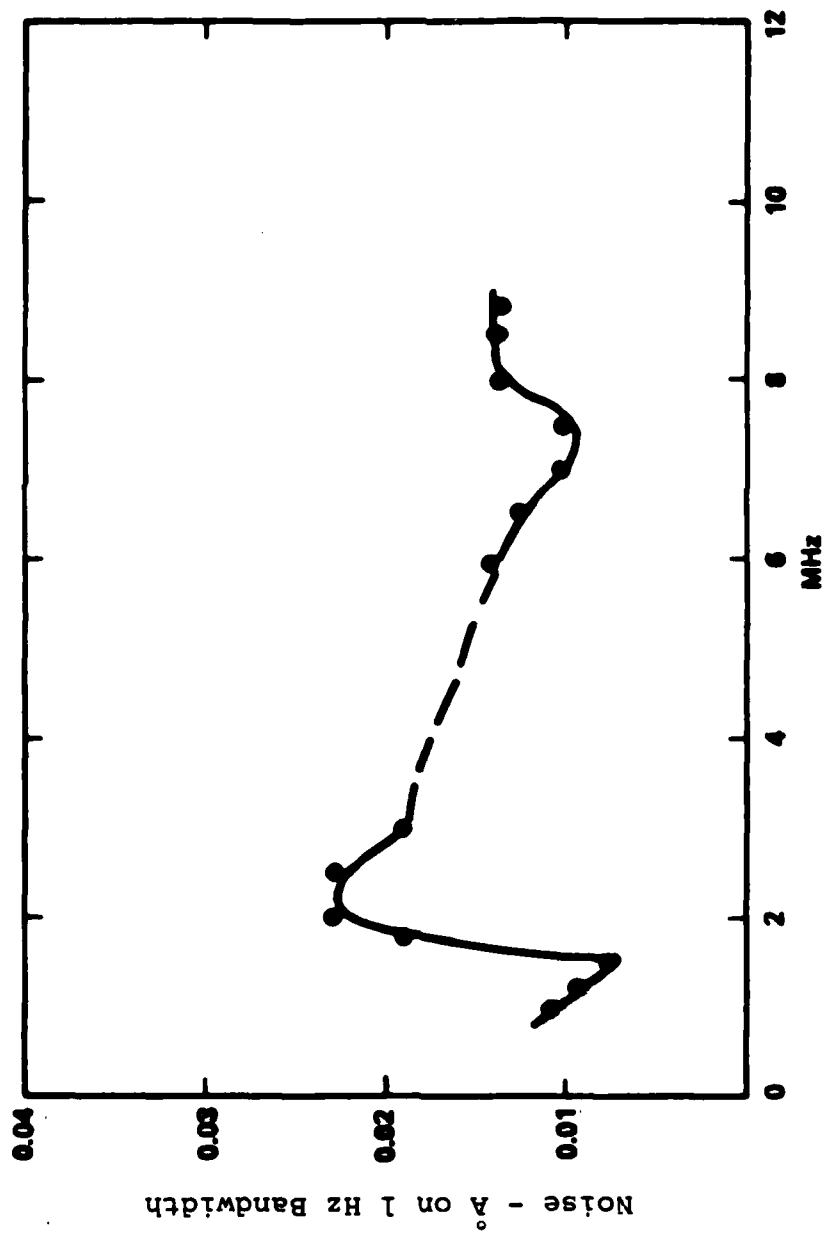


FIGURE 4. NOISE LEVEL OF LASER VIBROMETER.

## 5. FREQUENCY RESPONSE OF LASER VIBROMETER

The Laser Vibrometer was set up to look at the center of the face of a piezoelectric transducer, which was driven by an electrical signal of approximately 10 V rms. The response of the Laser Vibrometer was again measured with the PAR Lock-In Amplifier. The results, normalized to 1-V input, are shown in Fig. 5. They appear quite erratic, varying by 3:1 over the frequency range 1 to 12 MHz. The reason for this variation is thought to be the PZT transducer itself, which does not necessarily move as a rigid piston. Transverse modes are induced in the transducer so that the response at any one point varies with the mode structure. The transducer itself will appear much more uniform, since it averages over its whole face. The variations are then a consequence of making only single point measurements. Indeed, when the laser vibrometer was moved off the center of the transducer, the response was seen to vary markedly.

This situation can be resolved with a scanning version of the Laser Vibrometer, in which the whole mode structure of the face will be visible.

The response between 3 and 5 MHz is shown dotted because a signal generator was not available in this frequency range and therefore no measurements were made there.

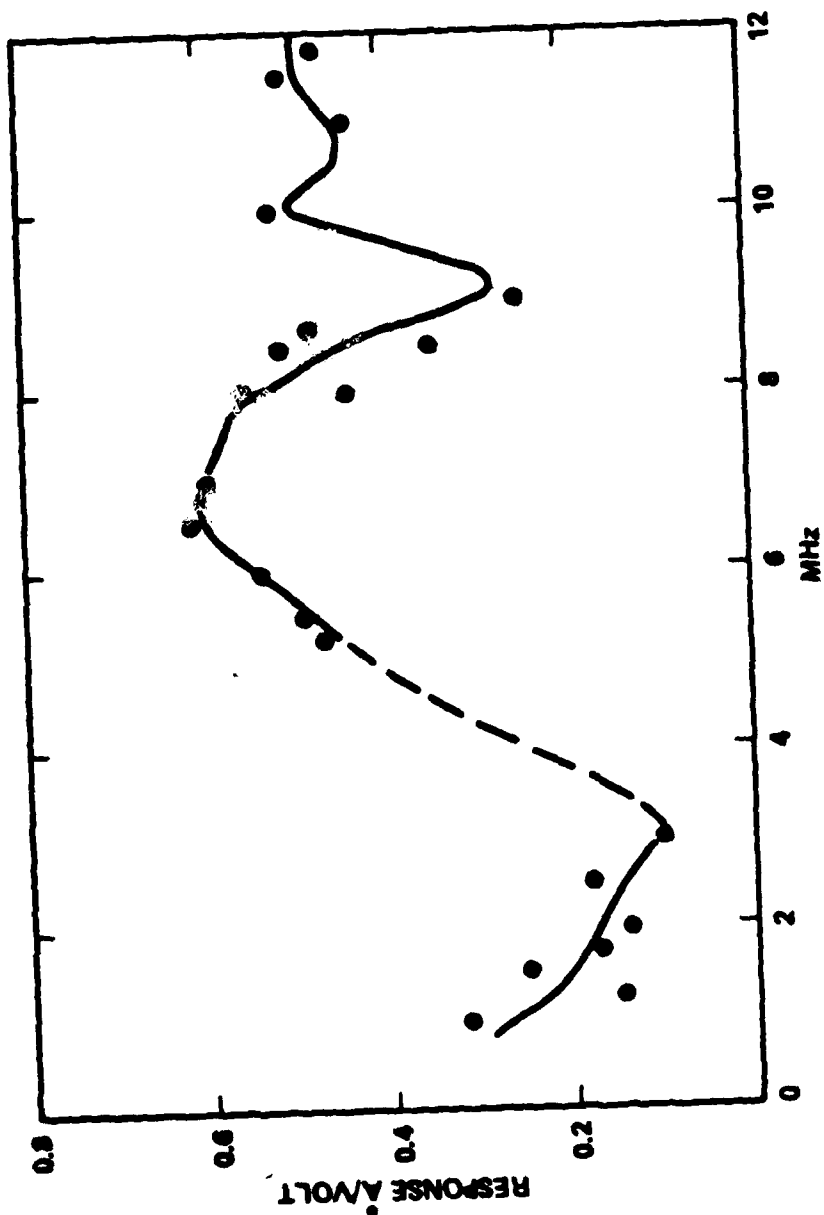


FIGURE 5. FREQUENCY RESPONSE OF LASER VIBROMETER MEASURING A PZT TRANSDUCER.

6. PULSE RESPONSE OF LASER VIBROMETER

A nominal 60-V, 50 nsec pulse was applied to the 10-MHz PZT transducer, and the output of the Laser Vibrometer was studied on an oscilloscope. The result, shown in Fig. 6, is the convolution of the response of the PZT transducer and those of the Laser Vibrometer. The response of the transducer was measured in the same way and is shown in Fig. 7. Both figures show oscillations with a frequency of 10 MHz, due to the finite bandwidth of the system.

NADC-79009-60

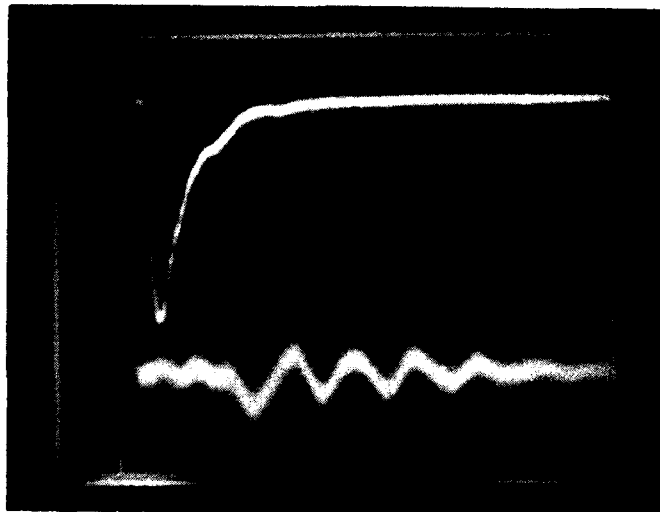


FIGURE 6. PULSE RESPONSE OF LASER VIBROMETER.

Time - 100 nsec/cm

Upper Trace - Electrical Input 15 V/cm

Lower Trace - Vibrometer Output 0.1 V/cm

NADC-79009-60

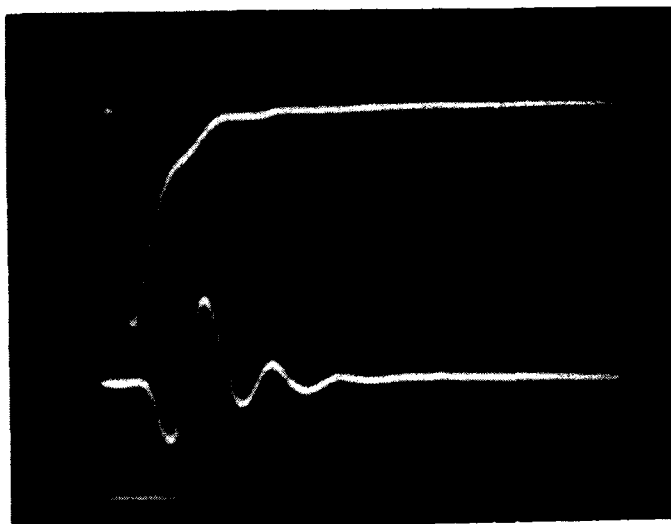


FIGURE 7. PULSE RESPONSE OF 10 MHz PZT TRANSDUCER.

Time - 100 nsec/cm

Upper Trace - Electrical Input 15 V/cm

Lower Trace - Transducer Output 0.5 V/cm

## 7. COMPARISON WITH PZT

It can be seen from Figs. 6 and 7 that in terms of signal-to-noise ratios, the PZT transducer is far superior to the Laser Vibrometer. The rms noise of the Laser Vibrometer was about 15 Å, whereas that from the PZT could not be measured with the Lock-in Amplifier. If the noise from the PZT transducer is thermal noise, then it corresponds to  $3 \times 10^{-3} \text{Å}$  on a 10-MHz bandwidth 5,000 times less than that for the Laser Vibrometer.

However we are not really comparing like with like here. The Laser Vibrometer makes measurements at a point, while the PZT transducer makes them over an area. This difference manifests itself in the frequency response of the PZT transducer, which is shown in Fig. 8. This PZT response was obtained by mounting two similar transducers face to face and measuring the output from the second transducer when the first was driven by a constant voltage. The gap between 3 and 5 MHz arose because the drive oscillator could not cover this range and no data was obtained. The response peaks at 8 MHz and drops off rapidly at lower and higher frequencies. This is a consequence of the backing of the PZT crystal, which makes it behave like an accelerometer at low frequencies.

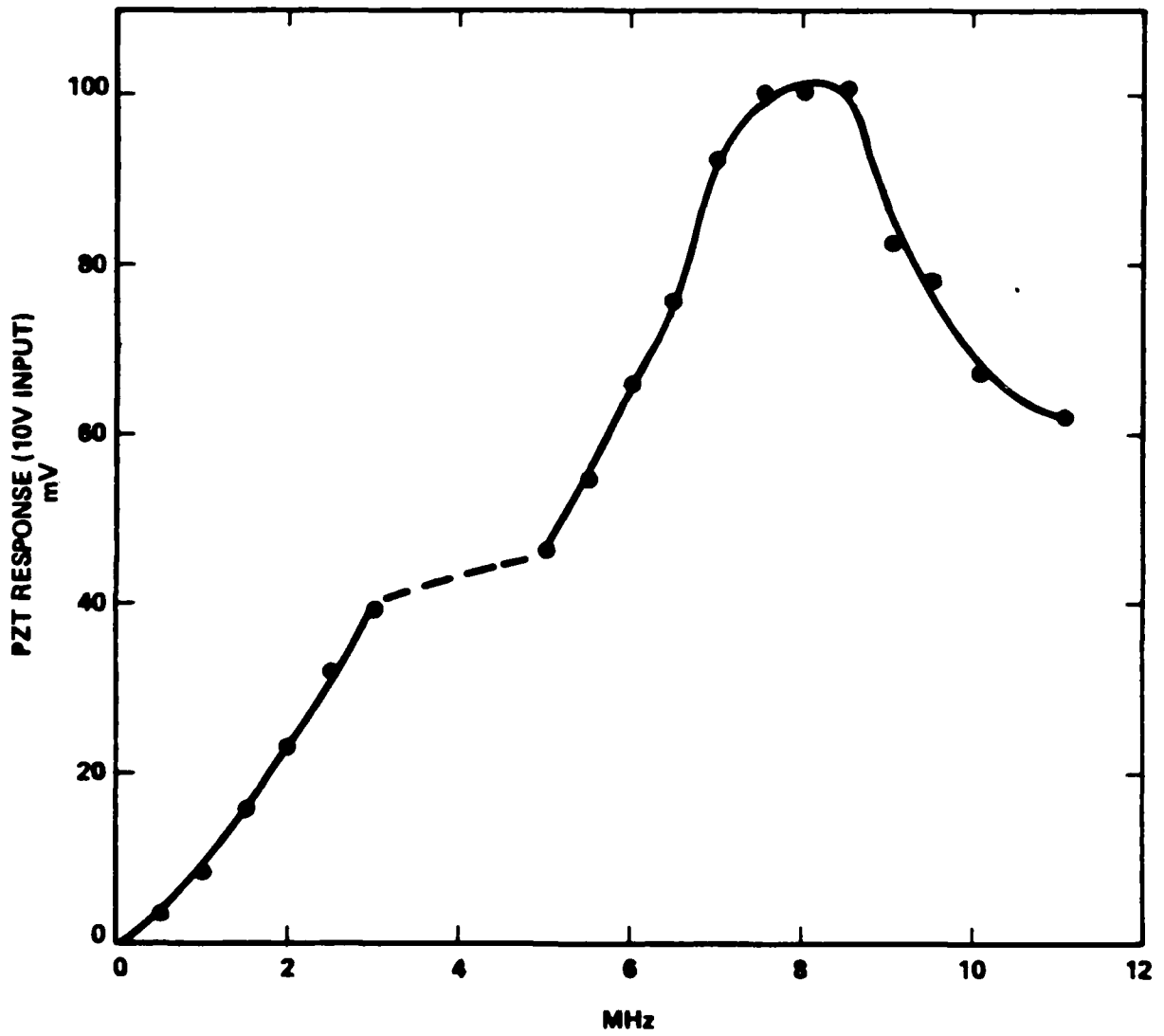


FIGURE 8. FREQUENCY RESPONSE OF PZT TRANSDUCER.

## 8. EFFECTS OF SURFACE FINISH ON SIGNAL-TO-NOISE RATIO

Table 1 describes the signal-to-noise ratio achieved with the Laser Vibrometer for different surface finishes. The signal levels quoted are for the 40-MHz carrier signal. The signal from a natural aluminum finish was so strong that it saturated the preamplifier of the photodiode. Other surfaces measured were a satin finish, matte white (paper) and black anodized aluminum. Even the last surface gave a respectable signal. Other surfaces, such as ground steel or aluminum spray paint, also were tried and found to work well.

All of these measurements were made at near-normal incidence. The best surface, natural aluminum, had a rapid reduction in signal strength at 5° to 10° off normal, whereas the matte white surface could go up to 45° off normal without a significant reduction in signal strength. Not surprisingly, the more diffuse surfaces worked at larger angles.

Most nonspecular surfaces worked well at distances up to 3 in., from the focusing lens, the longest tried.\* Specular surfaces were very sensitive to alignment and are not recommended.

---

\*Note: the distances in Figure 3 are from the laser end mirror and not the focusing lens.

TABLE I. SIGNAL STRENGTH AS A FUNCTION OF SURFACE FINISH.  
(Signal Levels mv rms.)

Distance (mm)	Surface Finish			
	Natural Aluminum	Satin Aluminum	White Matte	Black Aluminum
80	200*	55	40	20
40	200*	55	45	30
23	200*	65	40	47
8	200*	80	80	65
4	200*	75	80	70
3	200*	80	70	73

\*200 mv is maximum level that the preamplifier can deliver.

Noise level for all readings = 2.5 mv.

## 9. THEORETICAL PERFORMANCE OF THE OPTICAL SYSTEM

The mode of operation of the optical system is not at all obvious. For reasons discussed above, most of the optical power lies in the beam that is shifted by 40 MHz. This falls on the target. The focus is such that an image of the target is formed on the laser end mirror. The target is not at the focus of the laser beam but a little beyond it. The returned light comes in a cone around the +40 MHz beam. After reflection from the laser end mirror, it surrounds the -40 MHz beam. However, since the -40 MHz beam is not at the correct angle for the Bragg reflection, it has considerable amplitude modulation and hence is not suitable for a reference beam. The photodiode is therefore moved to one side of the beam, where stray scattered light provides the reference. By careful adjustment a "sweet spot" is found, in which there is virtually no amplitude modulation and sufficient light so that the avalanche photodiode is shot-noise limited. When this occurs, the resulting signal-to-noise ratio is

$$\frac{S}{N} = 10 \log \left( \frac{\eta P}{2h\nu\Delta f} \right) \text{ dB} ,$$

where  $h\nu$  = energy of a photon ( $3 \times 10^{-19}$  J),  $\Delta f$  = bandwidth ( $10^7$  Hz),  $\eta$  = quantum efficiency (0.6), and  $P$  = lesser of the signal or the reference beam power (in watts). Then

$$\frac{S}{N} = 10 \log P + 110 \text{ dB} .$$

The phase noise  $\Delta\phi$  of the phase detector is given by

$$\begin{aligned} \Delta\phi &= (N/S)^{\frac{1}{2}} \text{ radians} \\ &= (P \times 10^{11})^{-\frac{1}{2}} \text{ radians.} \end{aligned}$$

Thus for a signal power of  $10^{-7}$  watts, the phase noise on a 10 MHz bandwidth is 0.01 radians and  $3 \times 10^{-6}$  radians on a 1 Hz bandwidth, corresponding to an rms amplitude of 15 Å and  $4.8 \times 10^{-3}$  Å, respectively.

Table 2 shows the measured noise levels on both the full 50-MHz bandwidth of the photodetector and the 10-MHz bandwidth of the system. The top line is the measured noise level, which is primarily due to shot noise. This is about 20 dB more than the thermal noise of the detector, which is shown in the bottom line. There is significant shot noise due to illumination from room lights.

TABLE II. PHOTODIODE NOISE (300 mv = Full Scale = 158.2 nm or 5.27 Å/mv)

Bandwidth	50 MHz	10 MHz	Equivalent Displacement
Shot	2.75 mv	1.50 mv	~8.0 Å
Laser Off but room lights on	0.60 mv	0.35 mv	~1.5 Å
No lights Thermal noise only	0.27 mv	0.15 mv	~0.7 Å

The measured noise level of 1.5 mv on a 10 MHz bandwidth is equivalent to a noise power of  $1.5 \times 10^{-8}$  W. This NEP is generated by 35 μW of optical power. So we know that our reference beam is approximately 35 μW. Since the photodiode is dominated by shot noise there is little point in increasing the strength of the reference beam.

To generate an output signal of 200 mv, we require a signal of  $0.1 \mu W$  to mix with the reference beam. A stronger signal will saturate the preamplifier.

The amount of light collected from the target by the optical system is

$$P = P_0 Q d^2 / 4R^2 ,$$

where  $P_0$  = power in laser beam,  $Q$  = directivity of the surface,  $d$  = aperture of laser beam, and  $R$  = distance of focusing lens to the surface. The noise is then

$$\Delta\phi = \frac{R}{d} (P_0 Q)^{-1/2} \times 10^{-5} \text{ radians} .$$

Thus the noise increases as the distance of the target  $R$  increases, and decreases as the diameter of the laser beam increases.

From the discussion above,

$$P_0 \approx 10^{-7} \text{ watts} .$$

For  $P_0 = 3 \times 10^{-3}$  watts and  $\frac{R}{d} = 100$  (80 mm working distance), and  $Q = 1$ ; then  $P = 3.7 \times 10^{-7}$  watts. This power is about 15 times greater than that which is actually observed, and is attributable to two sources:

1. Optical losses in the system
2. Loss of coherence due to the surface roughness.

These two factors probably are comparable in magnitude.

## 10. IMPROVEMENTS IN SENSITIVITY

There are two ways in which the sensitivity of the Laser Vibrometer can be increased:

1. For strong signal cases, prevent the photodiode preamplifier from saturating
2. For weak signal cases, increase the collection angle for the backscattered light.

The first case applies to signals from aluminum surfaces, where at most distances measured, the signal is limited to 200 mv rms. By substituting a regular photodiode for the avalanche photodiode currently used, we can increase the signal-to-noise ratio from the current 40 dB to 60 dB or more. This will reduce the noise on a 10-MHz bandwidth from 15 Å to 1.5 Å rms or less.

The second case applies to matte surfaces from which the signal has been seen to decrease with distance. The collection angle can be increased by expanding the laser beam before it is focused on the target. The beam can be readily expanded by a factor of 5, giving an improvement of a factor of 5 in the noise level. Perhaps more important, the operating distance is increased by a factor of 5 for the same noise level.

## 11. CONCLUSIONS

We have successfully demonstrated the use of a laser interferometer for the detection of ultrasound. The instrument operated well up to distances of 80 mm, the maximum tried. The noise level was 15 Å rms on a 10-MHz bandwidth and 0.02 Å rms on a 1-Hz bandwidth. The instrument operated well on a wide variety of surfaces from aluminum to paper. The exception was a highly polished surface, which proved to be very sensitive to alignment. The best surfaces were satin aluminum or painted aluminum. In these cases, the signal-to-noise ratio was limited by saturation of the photodiode preamplifier.

A PZT transducer has a much better signal-to-noise ratio, but its response is much more restricted. Furthermore, the displacement of the transducer varies greatly across its face. Suggestions made to improve the performance of the Laser Vibrometer are: first, prevent saturation of the preamplifier by using a conventional rather than avalanche photodiode, and second, increase the collection aperture for the backscattered light. Since we are already-shot noise limited, increasing the laser power does not help the signal-to-noise ratio since the signal and the noise both increase together.

APPENDIX A: DESIGN OF THE PHASE TRACKER

INTRODUCTION

The basic system we have designed is indicated in Fig. A.1. It consists of a phase detector, which is stabilized by a phase lock loop (PLL). In this way small phase fluctuations with quite high bandwidth can be detected for further processing. What is presented here is a brief discussion of the circuit design.

AMPLIFIER

The amplifier simply receives the input signal and provides some gain and buffering. It consists of an LM 733 video amp with differential input to differential output. We provide for gain adjustment by a pot hooked to the emitters of the internal differential pair.

The output is also differential and with a DC term. The signal paths are DC decoupled by high pass RC components. Care must always be taken with a 733 to prevent oscillation at several hundred MHz. Often the oscillation cannot be seen on an oscilloscope but can be inferred from improper bias conditions.

PHASE DEMODULATOR

This consists of a MC 1496 double balanced modulator followed by a differential to single ended current buffer driving a low pass filter. The modulator multiplies the linear signal by a square wave reference ( $F_q$ ). This reference is an ECL signal swinging less than one volt. The linear gain of the modulator depends on the emitter resistor between pins 2 and 3.

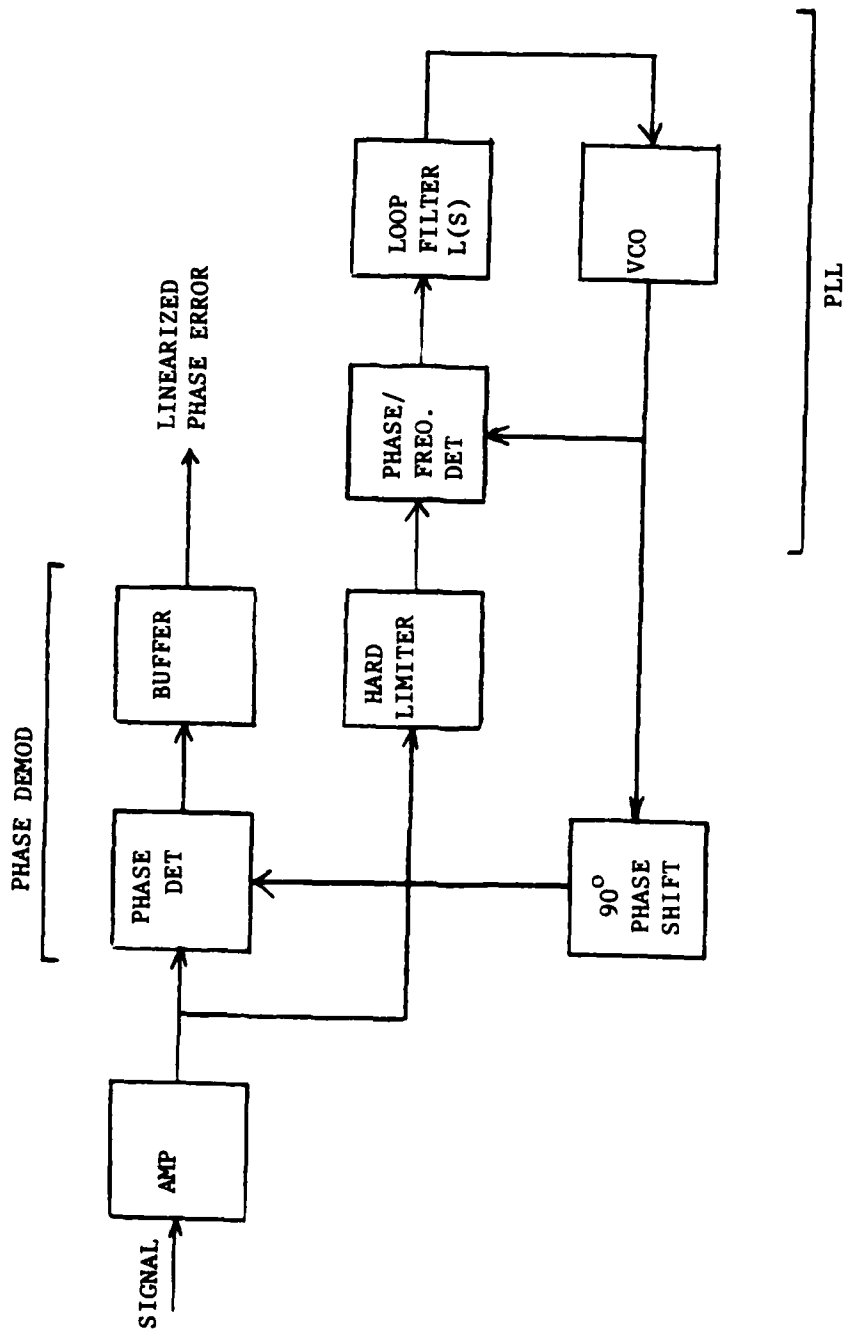


FIGURE A.1. BLOCK DIAGRAM OF THE PHASE TRACKER.

The current mode buffer injects the differential current signal at the emitters of two grounded base transistors (2N2907). One current flows through a current mirror before being summed with the other. Trimming the current bias allows us to zero the output.

The low pass filter is a three pole Butterworth with -3 dB frequency at 10 MHz. This should eliminate the undesired harmonics of the demodulation process. Thus it provides the upper frequency of the phase detection bandwidth.

#### HARD LIMITER

The hard limiter squares the signal using an MC 1651, which is an ECL comparator. Its output is converted to TTL logic levels by the MC 10125 for use by the PLL.

#### PHASE/FREQUENCY DETECTOR

This uses TTL gates as a set - reset flip flop. If one input to the detector has more positive transitions than the other then the flip flop remains longer in the 1 or 0 state. At phase lock both signals are at the same frequency and exactly out of phase resulting in equal 1 and 0 durations. For equal 1-0 dwell the phase detector is defined to have a "zero" output. The "phase offset" pot adds a negative bias to the linear network to translate the 50-50% duty cycle to a true zero output voltage. The three-pole low-pass Butterworth filter is used to remove high frequency terms and allow components below 1 MHz through to the rest of the loop.

There are some peculiarities to these types of phase-frequency detectors. One is a high frequency noise that causes the loop to jitter. The low pass filter removes this noise component. Next there are false lock frequency regions for this detector. The infinite gain of an integrator in the loop assure us of correct lock-in. Our principal concern is a "quiet" loop, since otherwise noise is added to the phase demodulator.

#### LOOP FILTER

The loop filter is selected to provide a rate tracking (velocity) servo. This is to compensate for frequency offsets in the reference oscillator and the rest frequency of the VCO. It also should prevent false lock of the phase/frequency detector. The loop transfer function is

$$L(S) = [1 + 1/RCS] = a_2 + a_1/S \quad (A-1)$$

given in Eq. (A-1). The RC is noted in the diagram. For analytic convenience the two constants  $a_1$ ,  $a_2$  are introduced.

The overall loop response is obtained by using the function  $a_0/S$  to represent the phase detector and VCO. This gives us a loop response in Eq. (A-2), where  $E(S)$  is the transfer function from input phase to loop phase error.

$$E(S) = \frac{S^2}{S^2 + Sa_2 a_0 + a_0 a_1} \quad (A-2)$$

The poles of this expression are approximately given in Eq. (A-3), where we are using a "slow" integrator term.

$$s_p = [a_0 a_2 - a_1/a_2] , - a_1/a_2 \quad . \quad (A-3)$$

That is, the frequency offset response embodied in the second term in Eq. (A-3) slowly responds to steps in frequency. The dominant pole is the "test" first term in Eq. (A-3). It is as though we have a first order loop but with a very slow velocity term that zeroes in on the frequency offset.

There is a voltage divider before and after the loop filter to allow us to adjust  $a_0$ . Note that the RC time constant sets the lowest pole.

#### VOLTAGE CONTROL OSCILLATOR (VCO)

The VCO is an LC oscillator tuned by changing the bias on a varactor diode. The rest frequency is tuned to be just below 80 MHz and the MC1200 divides the carrier frequency by two and converts from ECL to TTL. The oscillator chip MC 1648 is an ECL component with extremely wide band capability. A ferrite bead is used to suppress parasitic oscillations in the 100's of MHz. The "square adj" alters the AGC system of the chip to provide square wave output.

#### PHASE SHIFT

A 90° phase shift is obtained by inverting the 80 MHz signal and dividing by 2. Thus a quadrature wave is generated relative

NADC-79009-60

to the loop reference. The ECL signals  $F_q$  and  $\bar{F}_q$  drive the phase demodulator directly from the MCl200. With ECL signals a line run over one in. requires termination, which can be seen at the demodulator end.

D I S T R I B U T I O N L I S T

REPORT NO. NADC-79009 -60

	<u>No. of Copies</u>
NAVAIR (AIR-00D4)	8
(2 for retention)	
(1 for AIR-320)	
(1 for AIR-4114C)	
(1 for AIR-5163)	
(1 for AIR-5163B)	
(1 for AIR-51632)	
(1 for AIR-51632D)	
WPAFB, OH (AFWAL/LLP/MLLP) (Dr. Robert Crane)	1
NAVSHIPRSCHDEVCEN, Annapolis, MD (Code 2823)	1
NAVSURWPNCEN, Silver Spring, MD (D. Polansky), (J. F. Goff), (J. M. Warren)	3
Lockheed Missiles & Space Company, Inc., Sunnyvale, CA (Dr. M. I. Jacobson)	1
NRL, Washington, DC (S. Hart), (I. Wolock), (Dr. C. Sanday), (Dr. R. Weimer)	4
NAVSURWPNCEN, Dahlgren, VA (C. Anderson)	1
NAVAIRENGCEN, Lakehurst, NJ (D. Behmke, Code 92713), (P. Ciekurs, Code 92724)	2
University of Delaware, Newark, DE (Dr. R. B. Pipes) (R. Blake)	2
DTIC	12
DARPA, Arlington, VA (Dr. M. Buckley)	1
NAVSEC, Washington, DC (C. Craig)	1
Lawrence Livermore Laboratories, Livermore, CA (Dr. S. V. Kulkarni, Code L502)	1
NASA, Langley, Hampton, VA (Dr. J. Heyman)	1
NASA, Lewis Research Center, Cleveland, OH (A. Vary)	1
AMMRC, Watertown, MA (G. Darcy), (R. Brockelman)	2

DATE  
FILMED  
—8